Kharazmi University

Journal of Engineering Geology

Journal home page https://jeg.khu.ac.ir

OPEN ACCESS

Online ISSN 2981-1600

Experimental study on the performance of strip footings on geocell-reinforced granular slopes

Mohammadreza Harirsaz[1], Ali Ghanbari[2]✉, Gholamhossein Tavakoli Mehrjardi[3]

1. Research student, Department of Civil Engineering, Faculty of Engineering, Kharazmi University, Tehran,Iran. E-mail: std_harirsaz@khu.ac.ir
2. Professor, Department of Civil Engineering, Faculty of Engineering, Kharazmi University, Tehran,Iran. E-mail: ghanbari@khu.ac.ir
3. Associate Professor, Department of Civil Engineering, Faculty of Engineering, Kharazmi University, Tehran,Iran. E-mail: ghtavakoli@khu.ac.ir

Article Info

Article type:
Research Article

Article history:
Received 13October 2024
Received in revised form 20 December 2024
Accepted 28 December 2024

Keywords:
geocell, granular slope, plate load test, bearing capacity, coarse aggregates.

ABSTRACT

A series of reduced scale plate load tests was conducted to evaluate the bearing capacity of a strip footing resting on granular slopes. The effect of three factors including geocell burial depth, geocell length and spacing of geocell layers were discussed and evaluated. In this regard, 18 tests were performed to investigate the behavior of one and two layered geocell-reinforced slopes as well as the unreinforced slope and plain conditions. The results suggest that in single-layered geocell-reinforced slope, the optimum burial depth of the first layer of geocell reinforcement is 0.1 times of the strip footing width, whereas at greater depth beneficial effect of the geocell will reduce. In addition, expanding the reinforcement length up to approximately three times the foundation width could effectively increase the bearing capacity, whereas extending the length beyond that does not lead to any significant improvement. Furthermore, it was observed that use of two geocell layers by considering an optimum geocell space of 0.2 times of the foundation width could enhance the bearing capacity up to 226% in comparison with the unreinforced slope, and up to 79% of the plane condition for settlement ratio of 15%. Finally, the results indicate that the efficiency of the geocell reinforcements in lessening the gap between slope and plane conditions increases as the settlement of the footing rises due to better mobilization of dilation characteristics of granular backfill material and better lateral confinement of coarse aggregates in greater strains.

Introduction

In many cases, the foundations of structures are constructed in marginal ground conditions, which may bring about lack of bearing capacity. This can include the construction of buildings, roads in hilly regions and bridge abutments on the top of slopes. When a foundation is located on the top of a slope and subjected to footing loading, it will lead to a reduction in ultimate bearing capacity in comparison with the case that the foundation is constructed in plain condition. The decrease in bearing capacity depends on the location of footing on the crest, slope angle, and characteristics of the backfill material (Castelli and Motta, 2009; Chakraborty and Kumar, 2013; Keskin and Laman, 2014; JavanKhoshdel and Bathurst, 2015; Halder and Chakraborty, 2020; Chou et al., 2023).

The improvement of bearing capacity of these types of slopes is consequently one of the fundamental issues in foundation engineering practice since such structures are prone to slope failure. In recent years, researchers have reported beneficial effects of planar geosynthetic reinforcements to enhance bearing capacity of footings located near the edge of slopes

Cite this article: Harirsaz, M., Ghanbari, A., Tavakoli Mehrjardi, G.H. (2024). Experimental study on the performance of strip footings on geocell-reinforced granular slopes. Journal of Engineering Geology, 18 (5), 664-680. https//doi.org/10.22034/JEG.2024.18.5.10394

Publisher: Kharazmi University.
DOI: https//doi.org/10.22034/JEG.2024.18.5.10394

(Bathurst et al., 2003; EL Sawwaf, 2007; Alamshahi and Hataf, 2009; Halder and Chakraborty, 2018; Tavakoli Mehrjardi et al., 2016; Moradi et al., 2019; Kakrasul et al., 2020; Liu et al., 2021; Nazari et al., 2025). These investigations have indicated that geosynthetic reinforcements can enhance both the ultimate bearing capacity and the settlement characteristics of the foundations. However, geocell confinement in three dimensions better minimizes the lateral and vertical movements of the soil particles compared to the geogrids and geotextiles. Considerable investigations have been done on the geocell-reinforced foundations in the literature due to their extensive applications in the field of engineering (Dash et al., 2001; Madhavi Latha et al., 2008; Moghaddas Tafreshi and Dawson, 2010a; Dash, 2012; Neto, 2019; Tabatabai et al., 2019; Tavakoli Mehrgardi et al., 2019). The parameters influencing the performance of geocell-reinforced foundations and their optimum aspect ratios reported in previous studies are presented in Table 1.

Several studies have investigated the mechanisms and failure modes of the geocell-reinforced retaining walls and slopes. Mehdipour et al. (2017) and Khorsandiardebili and Ghazavi (2021) provided an analytical approach to calculate the safety factor of geocell-reinforced slopes. Also, Ardakani and Namai (2021) performed a numerical study to evaluate the behavior of geocell reinforced slope using FLAC 3D. Chen and Chiu (2008) investigated the behavior of geocell-reinforced retaining walls. Their findings suggested that when the reinforcement was embedded in the lower zone of the backfill, the wall's upper part displaced more than the lower part. Chen et al. (2013) showed that the failure modes of the gentler geocell-reinforced walls consist of a few slides passing along the interface between geocell layers, while that of the steep vertical walls revealed both modes of interlayer sliding and overturning failure. Song et al. (2018), via centrifuge model tests, found that when the slope inclination is relatively large, the sliding wedge propagates near the slope crest.

Calculation of the bearing capacity of a strip footing resting on the geocell-reinforced granular slopes is an applied problem in geotechnical engineering. Although several studies have been conducted to evaluate the behavior of the geocell-retaining walls under self-weight or surcharge, there are limited studies on the effect of footing loading on the stability of the geocell-reinforced slopes. Therefore, in this study, the effects of influential factors such as the burial depth of the first geocell layer in tandem with its length, as well as the effect of geocell space in double-layered geocell-reinforced slopes are evaluated.

Table 1. Effect of several parameters influencing the performance of geocell-reinforced foundations

Parameters	**Researchers**	**Optimimum value**	**Footing type**	**BCR**	**Geocell geometry**
Pocket size(d_g)	Dash et al. (2004)	0.8 to 1*D*	Circular	7	Chevron pattern
Particle size	Tavakoli Mehrjadi et al. (2016)	d_g/D_{50}=12-18 D/D_{50}=13-27	Circular	5	Non-circular shape
Relative density of backfill (D_r)	Dash (2010)	70%	Strip	-	Chevron Pattern
Width of Geocell mattress(b)	Latha and Rajagopal. (2007)	*b/B*=4-6	Strip	-	Chevron pattern
Height of Geocell mattress(H)	Moghadass Tafreshi and Dawson (2010a)	*H/B*=1.33	Strip	3	Non-circular shape

Cover thickness (u)	Dash et al. (2001)	0.1	Strip	4	Chevron pattern
Aspect ratio	Dash et al. (2001)	*h*/*d*=1.67	Circular	-	Chevron pattern

Test materials

Backfill material

The soil used in this study as backfill material was uniformly graded soil with medium particle size (D_{50}) of 7 mm. Fig.1 also shows the grain size distribution of this soil. The technical properties of the soil, classified as GP in the Unified Soil Classification System (ASTM D2487-11), are provided in Table 2.

Geocell

The Geocell used in the tests, made of heat-bonded non-woven geotextile, had pocket size of 110mm×110mm and height of 50 mm, respectively. The pockets of geocell have a non-circular shape (See Fig. 2). As a result, the pocket size (d_g) is defined as the diameter of an equivalent circular area (d_g=110mm). Fig. 2 illustrates a prototype view of the backfill materials and geocell. The engineering characteristics of the geocell are tabulated in Table 3.

In order to mobilize a greater value of friction angle on the Geocell-grain interface, coarse aggregate fill materials in addition to medium-dense fill condition are required. This matter has been confirmed by several researchers (Manju and Madhavi et al. 2013, Tavakoli Mehrjardi and Motarjemi 2018, Tavakoli Mehrjardi et al. 2019). The ratio of the geocell diameter cell size to the medium soil (d_g/D_{50}) is about 16. Also, the ratio of the loading plate diameter to the medium backfill size (D/D_{50}) is 21. This complies with the criterion recommended by Tavakoli Mehrjardi et al. (2019), as shown in Table 1. Fig. 3(b) shows the schematic of the physical test setup and its attachments consisting of a testing tank, loading system, and data measurement system. The dimensions of the test box are chosen in such a way that the boundary conditions do not affect the test results. This assumption was confirmed based on laboratory evidence during the experiments.

The monotonic loading system consisted of a hand-operated hydraulic jack and pre-calibrated load cell mounted on a steel strip plate, with 650 mm in length, 150 mm in width, and 30 mm in thickness, hand-operated hydraulic jack and pre-calibrated load cell mounted on a steel strip plate, with 650 mm in length, 150 mm in width, and 30 mm in thickness.

Table 2. Physical properties of backfill material

Description	value
Coefficient of uniformity, C_u	2.12
Coefficient of curvature, C_c	1.13
Effective grain size, D_{10}(mm)	3.52
Medium grain size, D_{50}(mm)	7
Moisture content (%)	2
Maximum dry density (kN/m^3)	16.64
Minimum dry density (kN/m^3)	13.62
Specific gravity	2.57
Friction angle at $D_r = 70\%$ (degree)*	45

* Obtained by direct shear test

In this study, the edge distance (D) of $0.5B_m$ was selected, which remained unchanged in all the tests, ensuring that the footing is close enough to the slope edge, which necessitates the use of soil reinforcement. The hydraulic jack applied the loading via a pre-calibrated load cell with a capacity of 10000 kg and an accuracy of ±0.02% of full scale. Dash (2010) showed that the beneficial effect of the geocell reinforcement was optimum when the relative density of the foundation soil was 70%. Consequently, all the model-footing tests were performed with the relative density of 70%. In all tests, firstly, soil embankment with the plane surface was constructed in layers of 50 mm thickness to reach 500 mm height. The weight of the soil required to fill each layer was calculated and placed in each layer separately. A small compactor was used to achieve the soil relative density of 70%. Besides, the moisture contents of the backfill, just before the loading, were also measured around 2%.

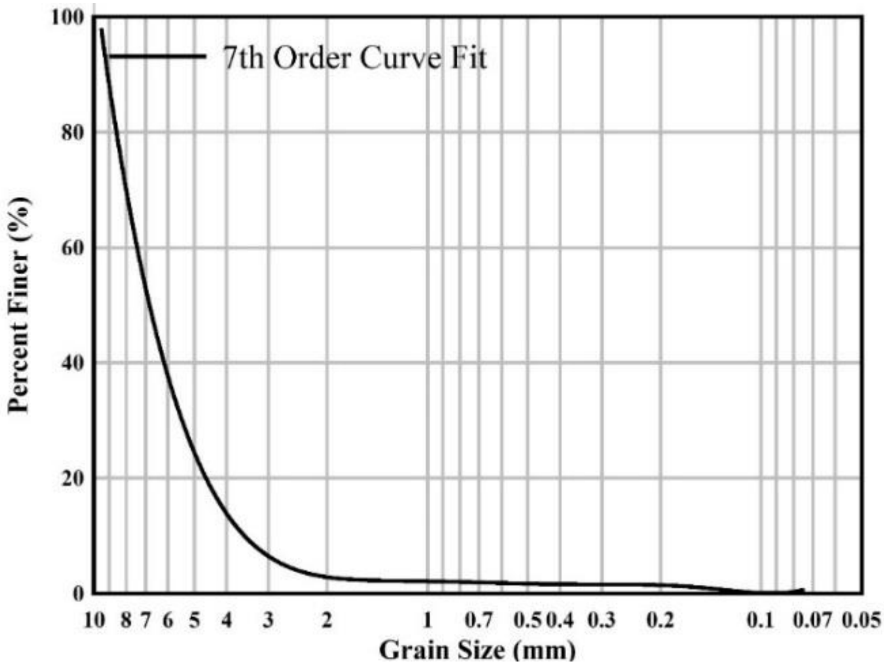

Fig. 1. Particle size distribution curve of the soil used beneath the footing

Table 3. Technical characteristics of the geocell

Description Value	value
Type of geotextile	Non-woven
Area weight ($^{kg}/_{m^3}$)	0.47
Maximum Tensile strength* ($^{kN}/_{m^3}$)	13
Elongation at max strength* (%)	55
Effective opening size* (mm)	0.07

*These values are related to the geotextile used in geocells.

The preparation of the unreinforced bed continued until reaching the level of reinforcements, after which the geocell reinforcements were placed, and the pockets of geocells were filled with a predetermined amount of soil mass. In order to better assess the backfill compaction, in some installations and after backfill placement, soil densities were measured according to ASTM D1556-07. The measured relative densities in all experiments were close enough to 70%. The thickness of soil cover (u) considered in the current study to prevent the damage of geocell walls under footing loads is 0.1B. According to Moghadass Tafreshi and Dawson (2010b), for obtaining optimal performance of geocell reinforcement, the thickness of the soil cover should be within the range of 0.05–0.1 times the footing size (D). After reaching the footing level, the steel strip plate was placed on the bed in its specific location. Halder and Chakraborty (2018) showed that when a strip footing is located on a slope as the slope angle increases, the effectiveness of the reinforcement in enhancing the bearing capacity of the footing increases as well. Therefore, a slope angle of 〖40〗 ^°was selected, noting that scale effect difficulty was the major obstacle for not selecting the slope angle less than 〖40〗 ^°. Fig. 3(a) shows the geometry of the slope backfill. The embankment was trimmed to achieve a slope backfill with an angle (α) of 〖"40" 〗 ^"°" .The soil beyond the slope face was gently excavated by a small shovel to achieve a slope backfill with an angle of 〖"40" 〗 ^"°" . The excavation was initiated far from the slope face to minimize the chance of variation of the relative density of the soil beneath the foundation as well as the soil near the slope face. Tavakoli Mehrjardi et al. (2016) also used the same technique for trimming the embankment to achieve slope's backfill with an angle of 〖45〗 ^°.The sequence of sample preparation is illustrated in Fig. 5. During the tests, monotonic loading was applied incrementally to reach the maximum attainable pressure.

The load was maintained until the footing settlements reached a plateau. Throughout the tests, to investigate any possible rocking or tilting of the footing, settlements were monitored by two dial gauges with an accuracy of 0.01% of the full range (50 mm), located on opposite edges of the loading plate. Similarly, an average of the recorded values were reported as the settlement of the footing at each loading step.

Fig. 2. A view of installed geocell in the backfill

Experimental testing program

In order to investigate the impact of geocell reinforcements on the response of the strip footing situated on the sloped backfill, a testing program was established. In this regard, 18 experimental tests were performed to examine the behavior of geocell-reinforced slope using one and two layers of reinforcement as well as the unreinforced slope conditions. In addition to the unreinforced slope test, to make a better assessment of the reinforcement effectiveness on slope stability, an unreinforced plane backfill was constructed and tested.

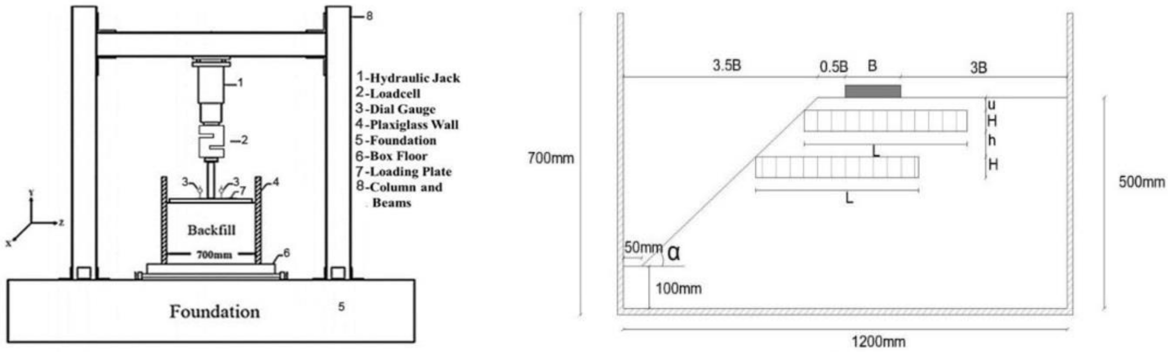

(a) (b)

Fig. 3. Schematic representation of the test setup (a) Y-Z section, and (b) X-Y section (Not to scale)

According to Table 4, in reinforced models, the variable parameters involved the burial depth of geocell (u), length of the geocell layers (L), and vertical distance between the first and second layers of geocell (h). Four burial depths including 0.1B, 0.2B, 0.4B, and 0.6B as well as three reinforcement lengths of 2.2B, 2.9B, and 4.4B were chosen where "B" is the width of the loading plate.

It should be clarified that the first step was the determination of the optimum depth(u_{opt}) and length (L_{opt}) of the geocell in the single-layered geocell reinforced slope. Afterwards, it was attempted to find the optimum value of the vertical distance between the second and first layers of geocell (h) to define an efficient performance for the double-layered geocell reinforcement.

(a) Unreinforced bed

(b) Installation of geocell

(c) Positioning strip plate

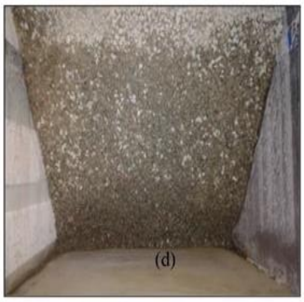

(d) Building the slope

(e) Finalized slope model

Fig. 5. Test bed preparation sequence

Moreover, in order to assess the utility of the apparatus, the accuracy of the measurements, the repeatability of the system, the reliability of the results and to verify the consistency of the test data, a few tests described in Table 4 were repeated at least twice. A close match between two experiments was observed.

Fig. 4. Assembly of the shaft and the base plate installed on the footing

Results and discussion

In this section, the bearing capacity of the footing located on the slope, bearing capacity ratio (BCR), slope influence factor $(IS)_u$, are discussed and evaluated.

Single-layered geocell reinforcement

Fig. 6 illustrates the response of the footing situated on the one-layer reinforced slope by considering burial depths and lengths of reinforcements. It can clearly be seen that the response curves of reinforced slopes were positioned between the unreinforced slope (as a lower limit) and the unreinforced plane backfill (as an upper limit). An important challenge is the question of how much the improvement technique is effective in enhancing slope stability. Therefore, it is necessary to compare the ultimate stresses of footing in "slope" and "plane" statuses. Consequently, the factor of slope influence $(IS)_u$ is defined by Eq. (1), where, $(q)_p$ and $(q)_i$ are the bearing pressure of "plane" and "slope" backfills, respectively.

$$(IS)_u = \frac{(q)_i}{(q)_p} \quad (1)$$

Table 4. Testing program

Test conditions	Test configuration	u/B	L/B	h/B	No of tests
Unreinforced	Plane	-	-	-	1+1[a]
	Slope	-	-	-	1+1[a]
Geocell reinforcement	Single-layered	0.1, 0.2, 0.4, 0.6	2.2, 2.9, 4.4	-	12+6[a]
	Double-layered	u_{opt}	L_{opt}	0.1, 0.2, 0.3, 0.4	4+1[a]

[*] The tests which were performed twice to confirm the repeatability of the test

Table 5 summarizes parameters of slope influence at footing's settlement of 0.05B,0.10B, and 0.15B for the case when one layer of geocell was used. According to Table 5, as can be expected, the footing located near the slope edge witnessed a clear reduction of the bearing capacity in comparison with the plane status. As the settlement of the footing increases the failure planes approach the slope edge, leading to a greater gap between the bearing capacity of the slope and the respective value for the plane condition. In the cases of reinforced slopes, the geocell walls surrounding the soil restrict the lateral deformations of soil particles inside them by tolerating tensile forces through their planes. In other words, when the failure plane crosses the geocell layer, the anchoring force provided by the reinforcement layer withstands the available driving forces so that, in turn, it makes the failure wedge form more voluminous than in the unreinforced slope, leading to a reduction of the bearing capacity gap between slope and plane conditions. To investigate the effect of the burial depth and the length of the reinforcement layer, bearing capacity ratio (BCR), according to Eq.(2), is defined as the ratio of the ultimate bearing capacity of footing on the reinforced slope ($(q_u)_{Re}$) to that on the unreinforced slope ($(q_u)_{Ur}$). Indeed, BCR describes how reinforcement can improve the performance of slope. The next section discusses the sensitivity of the whole system to the aforementioned parameters.

$$BCR=\frac{(q_u)_{Re}}{(q_u)_{Ur}} \qquad (2)$$

Effect of the burial depth of the geocell layers

The graph presented in Fig. 7(a) illustrates the variations of BCR versus various values of u/B. As a general trend, it can be clearly seen that BCR has declined with increasing the burial depth of the geocell layer. It means that when the geocell layer was located near the surface, the positive effect of reinforcement could be more significant. This can be because increasing the burial depth of the geocell makes the foundation more deformable due to the increasing unreinforced depth of backfill, leading to the formation of the slide zone over the geocell layer. In this respect, Chen and Chiu (2008) showed that for the case where the lower zone of the wall was reinforced with geocell, the slip plane appeared only in the upper zone and seemed incapable of penetrating through the reinforced lower zone. Several researchers have reported that the positive effect of the geocell layer was greatest when located at the depth of 0.1B the width of the footing (Dash et al., 2001; Dash et al., 2007; Dash et al., 2008; Moghaddas Tafreshi and Dawson, 2010a). Furthermore, Neto et al. (2013) proposed that the depth of the geocell layer placement must be smaller than 0.2B. As can be seen in the table 5, $(IS)_u$ factor of reinforced slope cases experiences a more significant increase as the settlement ratio increases. As an example, for S/B=0.05 $(IS)_u$ yields 0.57 for the unreinforced model. For u/B =0.1 and L=2.9 B, $(IS)_u$ reach 0.71, whereas the correspondence increase in the slope influence factor is 0.19 for S/B=0.1 and 0.24 for S/B=0.15.This can be explained by the fact, that in larger settlements more pressure will be exerted on the soil beneath the footing, whereas the geocell layer leads to more uniform pressure distribution on the underlying layers, thus enhancing the ultimate bearing capacity more effectively.

Based on the results acquired in this study, the most logical value for u/B is considered 0.1, enhancing the chance of success in backfill stability.

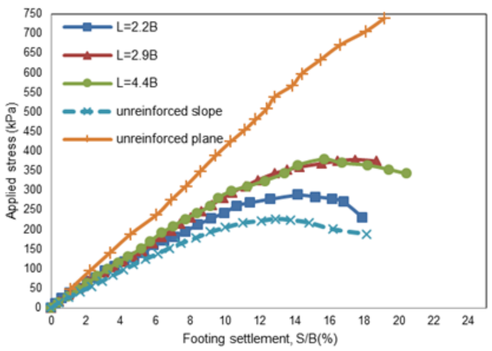

(a)

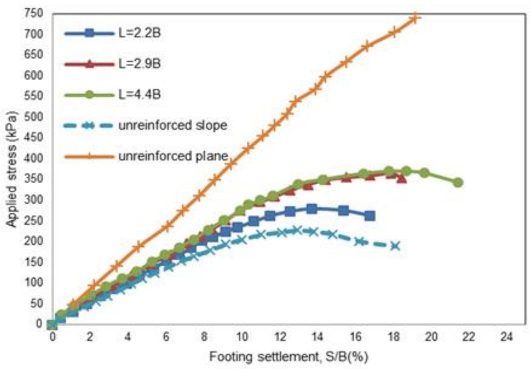

(b)

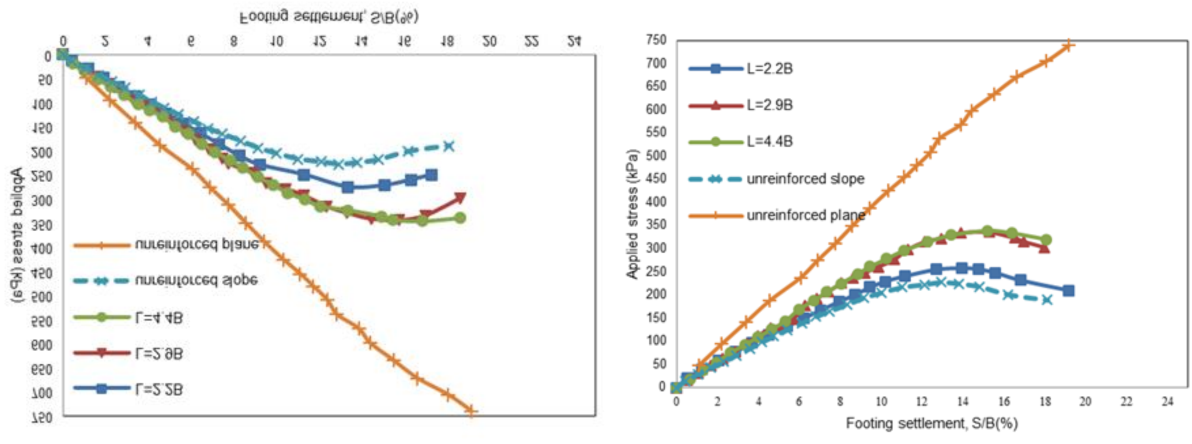

(c) (d)

Fig. 6. Variations of footing settlement versus applied pressure for unreinforced and single-layered geocell-reinforced slope (a) u=0.1B, (b) u=0.2B (c) u=0.4B, (d) u=0.6B

Effect of the length of the geocell layers

Fig. 7(b) depicts the variations of *BCR* for different lengths of the geocell layers. As can be seen, *BC*R has climbed to the value of 1.73, with increasing reinforcement length from 2.2*B* to 2.9*B*, due to the elevated active anchored length of the geocell. As the length of the geocell increases, so does the anchorage length, providing an opportunity for the formation of a deeper failure wedge and enhancing the slope stability. Likewise, the increase in geocell length would result in redistribution of footing pressure over a wider area below the geocell, thus reducing backfill deformations. However, for all values of the burial depth of geocell, the bearing capacity ratio did not experience any significant increase beyond the length of about 2.9*B*. The geocell layer of width about 2.9*B* completely encapsulates the failure zone of the soil. Isik and Gurbuz (2020) showed that the pullout capacity of geocell reinforcement becomes almost constant as the number of cells exceeds three rows in the direction of pullout force. As a result of any increase in the reinforcement layer beyond 2.9*B*, the extra positive effect of geocell-anchored length behind the failure wedge would become insignificant, leading to a negligible improvement in the bearing capacity of the reinforced slope. It is worth noting that, Table 5 shows as the settlements exceed S/B=0.05 the positive impact of extending the geocell length from 2.2B to 2.9B on the $(IS)_u$ becomes more notable. To illustrate this, when S/B=0.05 for the slope with L=2.9B, u/B=0.1 configuration $(IS)_u$ equals 0.71 compared to 0.66 for the case with shorter reinforcement length (L=2.2B and u/B=0.1). Nevertheless, when S/B=0.1 the $(IS)_u$ yields 0.6 for the latter and 0.69 for the former case, it shows more obvious improvement as the settlement rises. Similarly, for S/B=0.15 the correspondence rise in $(IS)_u$ factor as a result of increasing length from 2.2B to 2.9B is more notable than S/B=0.1. It is noteworthy that Khalvati Fahliani et al. (2021) stated that the geocell back length larger than zero has a slight impact on boosting the footing's bearing stress at smaller settlement ratios (s/B < 20%). However, in the current study due to the presence of coarse soil grains inside geocells, the dilation of soil particles will result in better confinement of soil particles in larger settlements, leading to higher pullout capacity of the geocell layer. Conversely, when the geocell length increases from L=2.9B to L=4.4B, the increase in the reinforcement does not have any major influence in improving $(IS)_u$ factor as the settlement ratio increases. This can be explained by the fact that excessive geocell back length does not provide any additional pullout capacity since negligible stress will be transmitted to the length beyond the necessary anchorage length.

To sum up, the optimum length of the geocell of three times the footing width can be recommended when the loading plate is located at a distance equal to half of the footing width.

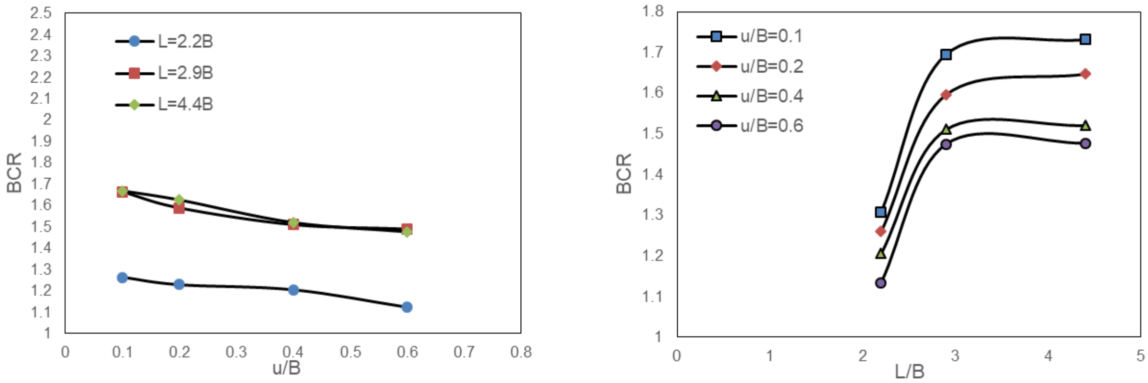

(a) (b)

Fig. 7. BCR variations with respect to change of (a) burial depth (b) length of geocell layers

Double-layered geocell reinforcement

According to the results presented in Table 5, although the single-layered geocell layer could enhance the bearing capacity of the unreinforced slope, arguably there is a significant gap between the response of the reinforced slope and unreinforced plane condition. In order to lessen this gap, double-layer geocell reinforcement was examined. Based on the findings of this study, to provide the best response in single-layered reinforcement, the burial depth and length of geocells should be 0.1B and 2.9B, respectively. Thereafter, the sensitivity of the system to various spaces between two layers of geocells was evaluated to find the most stable condition. Fig. 8(a) illustrates the response of the footing located on the double-layered reinforced slope by considering the space between the first and second layers of reinforcement. Table 6 reports the values for factors of slope influence at footing’s settlement of 0.05B, 0.1B, and 0.15B for the case when two geocell layers were used. It can be clearly seen that the response of the double-layered system has considerably improved in comparison with the single-layered reinforcement. For instance, when h/B was 0.2 for S/B=0.05, the bearing capacity of the reinforced slope will be almost equal to the plane condition, and the corresponding $(IS)_u$ values for S/B=0.1 and S/B=0.15 are 0.92 and 0.79, which are significantly higher than the equivalent values for the case L=2.9B, u/B=0.1 (Table 5). Fig.8(b) shows how the geocell layers space (h/B) affects the efficiency of the reinforced slope using the BCR factor. Interestingly, there is an extremum for the graph, confirming the existence of an optimum value for geocell space that is equal to 0.2B, yielding the highest value of BCR. Conceivably, On the one hand, when h/B=0.1 geocell layers are close to each other, due to the lack of interconnection between the layers, they do not show an integrated behavior.

Table 5. Factors of slope influence versus footing’s settlement (one layer reinforcement)

Settlement	Unreinforced slope	Single-layer reinforced slope			
		u/B	Reinforced(L=2.2B)	Reinforced(L=2.9B)	Reinforced(L=4.4B)
$(IS)_u$ S/B=5%	0.57	0.1	0.66	0.71	0.74
		0.2	0.64	0.69	0.71
		0.4	0.62	0.68	0.69
		0.6	0.61	0.66	0.67
$(IS)_u$ S/B=10%	0.5	0.1	0.6	0.69	0.70
		0.2	0.58	0.67	0.68
		0.4	0.57	0.66	0.67

		0.6	0.55	0.65	0.66
$(IS)_u$ S/B=15%	0.35	0.1	0.46	0.59	0.61
		0.2	0.44	0.57	0.57
		0.4	0.43	0.55	0.55
		0.6	0.41	0.54	0.54

Table 6. Factors of slope influence ($(IS)_u$ at S/B= 0.15B for double-layered reinforced slope

Settlement	Unreinforced slope	Double layer reinforced slope (L=2.9B, u=0.1B)			
		h/B=0.1	h/B=0.2	h/B=0.3	h/B=0.4
$(IS)_u$ S/B=5%	0.57	0.88	1	0.94	0.85
$(IS)_u$ S/B=10%	0.5	0.85	0.92	0.89	0.8
$(IS)_u$ S/B=15%	0.35	0.72	0.79	0.78	0.68

Noting that in this case, the small thickness of the soil layer between the first and second layers of geocell would prevent effective load distribution on the second layer of reinforcement. On the other hand, when h/B was larger than 0.2B, as the distance between the second layer and first layer increased, the material between the two layers was subjected to more displacement, thus increasing the possibility of the forming shear zone over the second layer would increase. In this regard, Yoon et al. (2008) and Moghaddas Tafreshi et al. (2013) reported that the effective vertical space of geocell layers was 0.2 times the plate diameter under plane conditions, while in the case of larger spaces between geocell layers, the efficiency of the reinforced system comparatively reduced.

Scale effect

The theory of dimensional analysis is summarized in Buckingham's theorem and is supported by the scaling laws proposed in the literature (Langhaar, 1951). The scale effects associated with the experimental model can be clarified through dimensional analysis. Several studies have used the dimensional analysis to investigate the effects of different parameters on the performance of the reinforced soil foundation beds (Fakher and Jones, 1996, Sireesh et al., 2009). The performance of a system in terms of physical modeling is directly dependent on geometrical matters and aspect ratios. In other words, the scale effect should be tested in the interpretation of the obtained results, especially when it applies to practical models. The major physical parameters influencing the response of geocell-reinforced slope systems can be summarized as B, D, u, h, α, L, D_r ,D_{50}, ø, c, γ, ν, n, E_{soil}, E_g ,d_g ,H_g; where α is the slope angle, D_r represents relative density of slope's backfill, ϕ, c, γ, ν, E_{soil}, and E_g are internal friction angle, cohesion, unit weight, Poisson's ratio, secant elastic modulus of the backfill, and elastic modulus of geocell, respectively. The function that governs the geocell reinforced slope systems can be written as Eq. (3).

$$q_u = (B,\ D,\ u,\ h,\ L,\ D_r\ .\ D_{50}\ .\ ø\ .\ c\ .\ \gamma\ .\ \nu,\ E_{soil}\ .\ E_g\ .\ d_g\ .\ H_g\ .\ \alpha) \quad (3)$$

The equation comprises 16 parameters with two fundamental dimensions (i.e., length and force). Hence, Eq. (3) can be reduced to 14 independent parameters ("π" _"1," "π" _"2," "π" _"3,…….." "π" _"14)" and substituted with Eq. (4)

$$\frac{q_u}{\gamma B}=(\frac{D}{B},\frac{u}{B},\frac{h}{B},\frac{L}{B}\, D_r,\, \frac{D_{50}}{B},\, \varnothing,\, \frac{c}{\gamma B},\, \frac{\gamma D_{50}}{E_{soil}},$$

$$\nu,\, \frac{E_{soil}}{E_g},\, \frac{d_g}{D_{50}},\frac{H_g}{B},\, \alpha) \quad (4)$$

A prototype footing (p) with a diameter n times that of the model (m), Eq. (5) can be considered as:

$$n=\frac{B_p}{B_m} \quad (5)$$

The π terms should be equal for both the model and prototype to maintain the similarity. As an example, if a strip footing with a width of 1.5 m is studied (i.e., n = 10), parameters D, u, h, L, D_{50}, d_g and H_g should be considered 10 times the model parameters. Assuming the soils used in the model and prototype have the same unit weight, then E_{soil} and E_g should be considered 10 times the model parameters. In this situation, Eq. (6) can be satisfied to obtain the bearing capacity of the prototype system. Noting that the above-mentioned dimensional analysis is limited for the elastic response of reinforcements. Otherwise, for the nonlinear behavior of reinforcements and depending on the transferred stress level in geocell, the relationships should be fully adjusted.

$$(\frac{q_u}{\gamma B})_m=(\frac{q_u}{\gamma B})_p \Rightarrow (q_u)_p=n(\frac{\gamma_p}{\gamma_m})(q_u)_m \approx n(q_u)_m \quad (6)$$

Conclusion

A series of plate load tests were conducted to evaluate the bearing capacity of a strip footing resting on the geocell-reinforced granular slopes. This experimental study examined the effects of key factors, including the burial depth of the first geocell layer in tandem with its length, as well as the effect of geocell space in double-layered geocell-reinforced slope to improve the slope response against the surface loadings near the crest. Based on this study, the following conclusions can be drawn:

- Geocell reinforcement was successful in increasing the bearing capacity of the slope due to providing anchorage length behind the failure wedge and reducing lateral deformations of the soil particles surrounded in the geocell pockets.
- The greatest improvement in the bearing capacity of the slope reinforced with one layer of geocell was observed when the geocell layer was placed at a depth of 0.1 times the footing width beneath the footing base. However, at greater depth beneficial effect of the geocell reduced as the failure planes tend to form above the geocell layer.
- The optimum vertical spacing between the first and second layers of the geocells, which resulted in the maximum ultimate bearing capacity is 0.2 times the width of the footing.
- For surface loading at a short edge distance, increasing the length of the geocell reinforcement by about three times the footing width boosts the bearing capacity. However, for the lengths beyond this value, the beneficial effect of geocell reinforcement would be insignificant.
- The positive impact of the geocell reinforcement in reinforcing the granular slope increases as the settlement ratio increases due to the mobilizing dilation characteristics of granular backfill material and better lateral confinement of soil grains by geocell in larger pressures.
- Provision of geocell reinforcement beneath the footing increases the bearing capacity of the footing by 173% and 226% compared to unreinforced slope for one and two layers of reinforcement, respectively.
- In the case both geocell layers are located at optimum depths with optimum lengths, geocell reinforcement is successful in enhancing the bearing capacity of slope up to 77% of the plane backfill capacity for S/B=0.15.

As with other studies, the results of this research were influenced by experimental conditions. For instance, the results were obtained for only one type of reinforcement, one type of soil, and one width of the footing. Specific applications should only be made after considering the above limitations. Nevertheless, this study provided insight into the basic mechanism that establishes the behavior of slope reinforced by geocell under static loads, which may be used to guide further studies.

References

Alamshahi, S., & Hataf, N. (2009). Bearing capacity of strip footings on sand slopes reinforced with geogrid and grid-anchor. Geotextiles and Geomembranes, 27(3), 217-226. https://doi.org/10.1016/j.geotexmem.2008.11.011

Ardakani, A., & Namaei, A. (2021). Numerical investigation of geocell reinforced slopes behavior by considering geocell geometry effect. Geomechanics and Engineering, 24(6), 589-597. https://doi.org/10.12989/gae.2021.24.6.589

ASTM D1556 (2007), Standard Test Method for Density and Unit Weight of Soil in Place by the Sand-cone Method.

ASTM D2487 (2011), Standard Practice for Classification of Soils for Engineering Purposes (Unified Soil Classification System), ASTM International, West Conshohocken, PA

Bathurst, R. J., Blatz, J. A., & Burger, M. H. (2003). Performance of instrumented large-scale unreinforced and reinforced embankments loaded by a strip footing to failure. Canadian Geotechnical Journal, 40(6), 1067-1083. https://doi.org/10.1139/t03-052

Castelli, F., & Motta, E. (2009). Bearing Capacity of Strip Footings Near Slopes. Geotechnical and Geological Engineering, 28(2), 187-198. https://doi.org/10.1007/s10706-009-9277-9

Chakraborty, D., & Kumar, J. (2013). Bearing capacity of foundations on slopes. Geomechanics and Geoengineering, 8(4), 274-285. https://doi.org/10.1080/17486025.2013.770172

Chen, R.-H., & Chiu, Y. (2008). Model tests of geocell retaining structures. Geotextiles and Geomembranes, 26(1), 56-70. https://doi.org/10.1016/j.geotexmem.2007.03.001

Chen, R.-H., Wu, C.-P., Huang, F.-C., & Shen, C.-W. (2013). Numerical analysis of geocell-reinforced retaining structures. Geotextiles and Geomembranes, 39, 51-62. https://doi.org/10.1016/j.geotexmem.2013.07.003

Chou NNS, Yang KH, Wu HM, Lin JJ, Ho SJ, & Liu CN. (2023). Case study of a reinforced soil slope with marginal backfill as a detention pond in flood control. Journal of GeoEngineering, 18(1), 033-047, http://dx.doi.org/10.6310/jog.202303_18(1).4

Dash, S. K. (2010). Influence of relative density of soil on performance of geocell-reinforced sand foundations. Journal of Materials in Civil Engineering, 22(5), 533-538. https://doi.org/10.1061/(ASCE)MT.1943-5533.0000040

Dash, S. K. (2012). Effect of geocell type on load-carrying mechanisms of geocell-reinforced sand foundations. International Journal of Geomechanics, 12(5), 537-548. https://doi.org/10.1061/(ASCE)GM.1943-5622.0000162

Dash, S. K., Krishnaswamy, N., & Rajagopal, K. (2001). Bearing capacity of strip footings supported on geocell-reinforced sand. Geotextiles and Geomembranes, 19(4), 235-256. https://doi.org/10.1016/S0266-1144(01)00006-1

Dash, S. K., Rajagopal, K., & Krishnaswamy, N. R. (2004). Performance of different geosynthetic reinforcement materials in sand foundations. Geosynthetics International, 11(1), 35-42. https://doi.org/10.1680/gein.2004.11.1.35

Dash, S. K., Rajagopal, K., & Krishnaswamy, N. R. (2007). Behavior of geocell-reinforced sand beds under strip loading. Canadian Geotechnical Journal, 44(7), 905-916. https://doi.org/10.1139/t07-035

Dash, S. K., Reddy, P. D. T., & Raghukanth, S. (2008). Subgrade modulus of geocell-reinforced sand foundations. Proceedings of the Institution of Civil Engineers-Ground Improvement, 161(2), 79-87. https://doi.org/10.1680/grim.2008.161.2.79

El Sawwaf, M. A. (2007). Behavior of strip footing on geogrid-reinforced sand over a soft clay slope. Geotextiles and Geomembranes, 25(1), 50-60. https://doi.org/10.1016/j.geotexmem.2006.06.001

Fahliani, H. K., Arvin, M. R., Hataf, N., & Khademhosseini, A. (2021). Experimental Model Studies on Strip Footings Resting on Geocell-Reinforced Sand Slopes. International Journal of Geosynthetics and Ground Engineering, 7(2), 1-15. https://doi.org/10.1007/s40891-021-00270-1

Halder, K., & Chakraborty, D. (2018). Bearing

Capacity of Strip Footing Placed on the Reinforced Soil Slope. International Journal of Geomechanics, 18(11), 06018025. https://doi.org/10.1061/(ASCE)GM.1943-5622.0001278

Halder, K., & Chakraborty, D. (2020). Probabilistic bearing capacity of strip footing on reinforced anisotropic soil slope. Geomechanics and Engineering, 23(1), 15-30. https://doi.org/10.12989/gae.2020.23.1.015

Isik, A., & Gurbuz, A. (2020). Pullout behavior of geocell reinforcement in cohesionless soils. Geotextiles and Geomembranes, 48(1), 71-81. https://doi.org/10.1016/j.geotexmem.2019.103506

Javankhoshdel, S., & Bathurst, R. J. (2015). Influence of cross correlation between soil parameters on probability of failure of simple cohesive and c-ϕ slopes. Canadian Geotechnical Journal, 53(5), 839-853. https://doi.org/10.1080/17486025.2013.770172

Kakrasul, J. I., Han, J., & Rahmaninezhad, S. M. (2020). Load-Deformation Behavior of Geosynthetic-Reinforced Retaining Walls with Limited Fill Space Under Static Footing Loading. Transportation Infrastructure Geotechnology, 7(3), 309-331. https://doi.org/10.1007/s40515-020-00132-9

Keskin, M. S., & Laman, M. (2014). Experimental study of bearing capacity of strip footing on sand slope reinforced with tire chips. Geomechanics & engineering, 6(3), 249-262. https://doi.org/10.12989/gae.2014.6.3.249

Khorsandiardebili, N., & Ghazavi, M. (2021). Static stability analysis of geocell-reinforced slopes. Geotextiles and Geomembranes, 49(3), 852-863. https://doi.org/10.1016/j.geotexmem.2020.12.012

Langhaar, J.L., (1951). Dimensional Analysis And Theory of Models. Wiley, New York, NY, USA.

Liu CN, Lin BH, Huang WW, & Ho YH. (2021). Finite element analyses of geosynthetic-reinforced soil ground under surcharge and probabilistic estimation of the bearing capacity. Journal of GeoEngineering, 16(3), 099-109. http://dx.doi.org/10.6310/jog.202109_16(3).3

Madhavi Latha, G., & Rajagopal, K. (2007). Parametric finite element analyses of geocell-supported embankments. Canadian Geotechnical Journal, 44(8), 917-927. https://doi.org/10.1139/T07-039

Madhavi Latha, G., Dash, S. K., & Rajagopal, K. (2008). Equivalent continuum simulations of geocell reinforced sand beds supporting strip footings. Geotechnical and Geological Engineering, 26(4), 387-398. https://doi.org/10.1007/s10706-008-9176-5

Manju, G.S., & Madhavi Latha, G. (2013). Interfacial friction properties of Geocell reinforced sand. International Journal of Innovative Research in Science, Engineering and Technology 2 (1), 25–31.

Mehdipour, I., Ghazavi, M., & Ziaie Moayed, R. (2017). Stability analysis of geocell-reinforced slopes using the limit equilibrium horizontal slice method. International Journal of Geomechanics, 17(9), 06017007. https://doi.org/10.1061/(ASCE)GM.1943-5622.0000935

Moghaddas Tafreshi, S.N., & Dawson, A. R. (2010a). Behaviour of footings on reinforced sand subjected to repeated loading–Comparing use of 3D and planar geotextile. Geotextiles and Geomembranes, 28(5), 434-447. https://doi.org/10.1016/j.geotexmem.2009.12.007

Moghaddas Tafreshi, S.N., & Dawson, A. R. (2010b). Comparison of bearing capacity of a strip footing on a sand with geocell and with planar forms of geotextile reinforcement. Geotextiles and Geomembranes, 28(1), 72-84. https://doi.org/10.1016/j.geotexmem.2009.09.003

Moghaddas Tafreshi, S.N., Khalaj, O., & Dawson, A. (2013). Pilot-scale load tests of a combined multilayered geocell and rubber-reinforced foundation. Geosynthetics International, 20(3), 143-161. https://doi.org/10.1680/gein.13.00008

Moradi, G., Abdolmaleki, A., & Soltani, P. (2019). Small-and large-scale analysis of bearing capacity and load-settlement behavior of rock-soil slopes reinforced with geogrid-box method. Geomechanics and Engineering, 18(3), 315-328. https://doi.org/10.12989/gae.2019.18.3.315

Nazari, R.A., Ghanbari, A. & Sharafi, H. (2025). An Earthquake-Induced Reinforced Slope Sliding Displacement Estimation Model Using a Probabilistic Procedure. Transp. Infrastruct. Geotech. 12, 72. https://doi.org/10.1007/s40515-024-00490-8

Neto, J. A. (2019). Application of the two-layer system theory to calculate the settlements and vertical stress propagation in soil reinforcement with geocell. Geotextiles and Geomembranes, 47(1), 32-41. https://doi.org/10.1016/j.geotexmem.2018.09.003

Neto, J.A., Bueno, B., & Futai, M. (2013). A bearing capacity calculation method for soil reinforced with a geocell. Geosynthetics International, 20(3), 129-142. https://doi.org/10.1680/gein.13.00007

Sireesh, S., Sitharam, T.G., & Dash, S.K., (2009). Bearing capacity of circular footing on geocell–sand mattress overlying clay bed with void. Geotextiles and Geomembranes. 27 (2), 89–98. https://doi.org/10.1016/j.geotexmem.2008.09.005

Song, F., Liu, H., Ma, L., & Hu, H. (2018). Numerical analysis of geocell-reinforced retaining wall failure modes. Geotextiles and Geomembranes, 46(3), 284-296. https://doi.org/10.1016/j.geotexmem.2018.01.004

Tabatabai Aghda, S. T., Ghanbari, A., & Tavakoli Mehrjardi, Gh. (2019). Evaluating the Applicability of Geocell-Reinforced Dredged Sand Using Plate and Wheel Load Testing. Transportation Infrastructure Geotechnology, 6(1), 21-38. https://doi.org/10.1007/s40515-018-00067-2

Tavakoli Mehrjardi, G. T., & Motarjemi, F. (2018). Interfacial properties of geocell- reinforced granular soils. Geotextiles and Geomembranes, 46(4), 384-395. https://doi.org/10.1016/j.geotexmem.2018.03.002

Tavakoli Mehrjardi, Gh., Behrad, R., & Tafreshi, S. M. (2019). Scale effect on the behavior of geocell-reinforced soil. Geotextiles and Geomembranes, 47(2), 154-163. https://doi.org/10.1016/j.geotexmem.2018.12.003

Tavakoli Mehrjardi, Gh., Ghanbari, A., & Mehdizadeh, H. (2016). Experimental study on the behaviour of geogrid-reinforced slopes with respect to aggregate size. Geotextiles and Geomembranes, 44(6), 862-871. https://doi.org/10.1016/j.geotexmem.2016.06.006

Yoon, Y. W., Heo, S. B., & Kim, K. S. (2008). Geotechnical performance of waste tires for soil reinforcement from chamber tests. Geotextiles and Geomembranes, 26(1), 100-107. https://doi.org/10.1016/j.geotexmem.2006.10.004

دسترسی آزاد

شاپا الکترونیکی ۲۹۸۱-۱۶۰۰

نشریه زمین شناسی مهندسی

Journal home page https://jeg.khu.ac.ir

دانشگاه خوارزمی

مطالعه آزمایشگاهی رفتار پی نواری بر شیب های مسلح شده با ژئوسل

محمدرضا حریرساز[۱] ، علی قنبری[۲]✉ غلامحسین توکلی مهرجردی[۳]

۱. محقق، دانشکده فنی و مهندسی، دانشگاه خوارزمی، تهران، ایران، رایانامه: std_harirsaz@khu.ac.ir

۲. استاد، دانشکده فنی و مهندسی، دانشگاه خوارزمی، تهران، ایران، رایانامه: Ghanbari@khu.ac.ir

۳. دانشیار، دانشکده فنی و مهندسی، دانشگاه خوارزمی، تهران، ایران، رایانامه: ghtavakoli@khu.ac.ir

اطلاعات مقاله

نوع مقاله: مقاله پژوهشی

تاریخ دریافت: ۱۴۰۳/۰۷/۲۲

تاریخ بازنگری: ۱۴۰۳/۰۹/۳۰

تاریخ پذیرش: ۱۴۰۳/۱۰/۰۸

کلیدواژه‌ها:

ظرفیت باربری، شیب، ژئوسل، مصالح دانه‌ای، طول مسلح کننده، تعداد لایه

چکیده

به منظور برآورد ظرفیت باربری پی‌های نواری بر روی شیب‌های مسلح شده با ژئوسل، تعدادی آزمایش بارگذاری صفحه انجام شده است. در همین راستا اثر مشخصاتی مانند طول لایه ژئوسل، تعداد و همچنین موقعیت قرارگیری آن‌ها بر ظرفیت باربری شالوده نواری واقع بر مصالح دانه‌ای که در مجاورت شیب قرارگرفته باشد بررسی‌شده است. نتایج این مطالعه نشان می‌دهد در حالتی که از یک لایه ژئوسل برای تسلیح استفاده شود عمق بهینه قرارگیری این لایه برابر با ۰/۱ عرض شالوده نواری است. همچنین افزایش طول مسلح کننده تا میزان ۳ برابر عرض می‌تواند ظرفیت باربری را افزایش دهد و افزایش طول مسلح کننده بیش از این مقدار تأثیر مثبت بیشتری در ظرفیت باربری ندارد و ممکن است باعث کاهش آن نیز بشود. از سوی دیگر استفاده از دو لایه ژئوسل می‌تواند باعث افزایش ظرفیت تا میزان ۱۲۶ درصد نسبت به حالت غیرمسلح گردد. لازم به ذکر است که شرط این موضوع قرارگیری ژئوسل در فاصله مناسب نسبت به لایه اول است که در این مطالعه برابر با ۰/۲ عرض شالوده نواری پیشنهاد شده است. در نهایت، نتایج نشان می‌دهد که کارایی تقویت شیب با ژئوسل در کاهش فاصله بین شرایط شیب و صفحه با افزایش نشست پی افزایش می‌یابد که دلیل آن بسیج بیشتر زاویه اتساع مصالح دانه‌ای شیب و محصور شدن جانبی بهتر سنگدانه‌ها در کرنش‌های بالاتر است.

مقدمه

قرارگیری شالوده بر روی زمین‌های فاقد ظرفیت باربری همواره یکی از مشکلاتی بوده است که مهندسین ژئوتکنیک با آن مواجه بوده‌اند. این موضوع به‌خصوص زمانی بیشتر موردتوجه قرار می‌گیرد که به دلایل مختلف مانند کمبود فضا شالوده در نزدیکی شیب واقع شده باشد. تحقیقات گذشته استفاده موفقیت‌آمیز ژئوسینتتیک‌ها مانند ژئوتکستایل و ژئوگرید را در چنین شرایطی تصدیق می‌کند. در سال‌های اخیر ژئوسل به دلیل عملکرد ویژه و تأثیر زیادی که در افزایش ظرفیت باربری خاک دارد موردتوجه قرارگرفته است. در این مطالعه اثر مشخصاتی مانند طول لایه ژئوسل، تعداد و همچنین موقعیت قرارگیری آن‌ها بر ظرفیت باربری شالوده نواری واقع بر مصالح دانه‌ای که در مجاورت شیب قرارگرفته باشد بررسی‌شده است.

مواد و روش ها

در این مطالعه اثر تغییرات پارامترهایی مانند طول لایه مسلح کننده تعداد آن‌ها و همچنین عمق قرارگیری لایه‌های مسلح کننده بررسی می‌گردد. برای بررسی تأثیر هر پارامتر لازم است تا سایر پارامترها ثابت نگه‌داشته شوند تا تغییرات ایجادشده تنها مربوط به یک پارامتر باشد. همچنین بایستی تعدادی آزمایش نیز بر روی خاک مسلح نشده نیز انجام گردد

استناد: حریرساز، م. ر.، قنبری، ع.، توکلی مهرجردی، غ. ح. (۱۴۰۳). مطالعه آزمایشگاهی رفتار پی نواری بر شیب های مسلح شده با ژئوسل. مجله زمین شناسی مهندسی، ۱۸ (۵)، ۶۸۰-۶۶۴. https://doi.org/10.22034/JEG.2024.18.5.10394

ناشر: دانشگاه خوارزمی.

تا بتوان به مقایسه رفتار خاک غیرمسلح و خاک مسلح شده با ژئوسل پرداخت.

برای انجام آزمایش‌ها از دستگاه بارگذاری صفحه استفاده می‌شود. ابتدا خاک را لایه‌لایه درون جعبه موردنظر ریخته و متراکم می‌شود تا به تراز قرارگیری مسلح کننده برسد. سپس مسلح کننده نیز را در داخل خاک قرار می‌گیرد و درون چشمه‌های آن را با خاک پرکرده و متراکم می‌شود و خاک‌ریزی را تا رسیدن به سطح نهایی ادامه می‌یابد. پس از ایجاد یک سطح صاف شیب با زاویه موردنظر ایجاد می‌شود. پس از آن نوبت به بارگذاری می‌رسد و در این حین باید رفتار و تغییرات ایجادشده در خاک ازجمله نشست و تغییر شکل‌های به وجود آمده در خاک و وقوع گسیختگی در خاک به‌دقت بررسی و ثبت شود . درنهایت بر مبنای نتایج حاصله و مقایسه با مطالعات قبلی رفتار خاک گزارش شده است.

بحث و نتایج

این مطالعه دربرگیرنده ۱۸ آزمایش شامل ۲ آزمایش غیرمسلح (حالت شیب‌دار و تخت) و همچنین ۱۲ آزمایش با یک لایه مسلح کننده و چهار آزمایش با دو لایه مسلح‌کننده است. هدف اصلی از انجام آزمایش‌ها بررسی اثر استفاده از ژئوسل بر افزایش ظرفیت باربری و کاهش نشست بستر زیر شالوده قرارگرفته در مجاورت شیب است. در این آزمایش‌ها اثر طول و عمق قرارگیری اولین لایه ژئوسل و همچنین فاصله دومین لایه ژئوسل با لایه اول بررسی شده است. بدین منظور یک سری آزمایش مسلح و غیرمسلح با استفاده از دستگاه بارگذاری صفحه انجام شده است که در آن‌ها از یک ورق فولادی با عرض ۱۵۰ میلی‌متر و طول ۶۵۰ میلی‌متر برای بارگذاری بر روی شیب استفاده شده‌است. اجزای مختلف دستگاه بارگذاری صفحه شامل باکس آزمایش، سیستم اعمال بار، سیستم اندازه‌گیری بار و تغییر مکان است.

نتیجه‌گیری

بر مبنای نتایج آزمایش‌ها و مشاهدات انجام‌شده می‌توان نتیجه گرفت که در حالتی که از یک لایه ژئوسل برای تسلیح استفاده شود عمق بهینه قرارگیری این لایه برابر با ۰/۱ عرض شالوده نواری است. همچنین افزایش طول مسلح کننده تا میزان ۳ برابر عرض می‌تواند ظرفیت باربری را افزایش دهد. این موضوع درصورتی است که افزایش طول مسلح کننده بیش از این مقدار تأثیر مثبت بیشتری در ظرفیت باربری ندارد و حتی می‌تواند باعث کاهش آن نیز بشود. نتیجه دیگر آن است که افزایش تعداد لایه‌های ژئوسل از یک لایه به دو لایه اغلب باعث افزایش ظرفیت باربری می‌گردد. لازم به ذکر است که شرط این موضوع قرارگیری ژئوسل در فاصله مناسب نسبت به لایه اول است که در این مطالعه برابر با ۰/۲ عرض شالوده نواری پیشنهاد شده است. علاوه بر این هرچه ژئوسل در اعماق بالاتر قرار داشته باشد نیروی بیشتری به آن می-رسد و در نتیجه سهم بیشتری از بار را تحمل می‌کند. همچنین هرچه عمق قرارگیری ژئوسل افزایش یابد از تأثیر مثبت آن کاسته خواهد شد زیرا سهم کمتری از بار به آن می‌رسد. در هر صورت استفاده از مصالح درشت‌تر باعث اندرکنش بهتر خاک و مسلح کننده می‌گردد و تأثیر مثبت استفاده از ژئوسل را افزایش می‌دهد. استفاده از یک لایه و دو لایه ژئوسل می‌تواند به ترتیب ظرفیت باربری را تا میزان ۹۵ و ۱۲۶ درصد افزایش دهد. همچنین در این حالت نسبت نشست (S/B) در لحظه گسیختگی از مقدار ۱۲/۹۱ برای حالت غیرمسلح به ۱۷/۴۷ برای حالت تسلیح تک لایه و ۱۹/۶۸ برای حالت تسلیح دولایه می‌رسد.